Metal-Induced Changes in the Fluorescence Properties of Tyrosine and Tryptophan Site-Specific Mutants of Oncomodulin†

Cindy M. L. Hutnik,‡,§ John P. MacManus,‡ Denis Banville,‖ and Arthur G. Szabo*,‡

Institute for Biological Sciences, National Research Council, Ottawa, Ontario, Canada K1A 0R6, and Biotechnology Research Institute, National Research Council, Montreal, Quebec, Canada H4P 2R2

Received December 17, 1990; Revised Manuscript Received April 12, 1991

ABSTRACT: Oncomodulin is a 108-residue, oncodevelopmental protein containing two calcium-binding sites identified as the CD- and EF-loops. The protein contains no tryptophan and only two tyrosine residues, one which is a calcium ligand in the CD-loop (Tyr-57) and one which lies in the flanking D-helix of this loop (Tyr-65). Site-specific mutagenesis was performed to yield five mutants, two with phenylalanine substituted for tyrosine in positions 57 and 65 and three with tryptophan substituted into position 57 in the CD-loop, position 65 in the D-helix, and position 96 in the EF-loop. The single Tyr-containing mutants demonstrated that position 57 was perturbed to a significantly greater extent than position 65 upon calcium binding. Although both tyrosine residues responded to decalcification, the fluorescence intensity changes were in opposite directions, with the more dominant Tyr-57 accounting for the majority of the intrinsic fluorescence observed in native oncomodulin. The substitution of tryptophan for each tyrosyl residue revealed that in both positions the tryptophan resided in polar, conformationally heterogeneous environments. The envrionment of Trp-57 was affected by Ca^{2+} binding to a much greater extent compared to that of Trp-65. Only 1 equiv of Ca^{2+} was required to produce greater than 70% of the Trp fluorescence changes in positions 57 and 65, indicating that Ca^{2+} binding to the higher affinity EF-loop had a pronounced effect on the protein structure. Substitution of Trp in place of lysine-96 at position 7 in the EF-loop showed that binding of the second Ca^{2+} equivalent in this mutant also affected the Trp-96 fluorescence when Tyr was also excited (λ_{ex} = 280 nm). This indicates that changes in the relative orientation of Tyr-57 and Trp-96 occurred when the CD-loop was filled.

The acidic calcium-binding protein oncomodulin is an oncodevelopmental protein possessing a number of unique and distinguishing properties (MacManus et al., 1985). Primary sequence analysis revealed that oncomodulin was a member of the superfamily of calcium-binding proteins and possessed greater than 55% identity of sequence with the β-parvalbumin subfamily (MacManus et al., 1983). Recently, the three-dimensional structure of oncomodulin has been solved and was found to be very similar to that of carp parvalbumin (Ahmed et al., 1990). Within both proteins, there exists a triad of helix–loop–helix structures with only two of them being functional in calcium binding. Despite a knowledge of its three-dimensional crystal structure and cellular prevalence, it is still not known if oncomodulin functions in vivo as a modulator protein and if it is associated with the observed changes in calcium-mediated growth control of neoplastic cells (MacManus et al., 1978; Whitfield et al., 1980; MacManus & Whitfield, 1983).

The purpose of this study was to examine in detail the nature of metal ion induced localized conformational changes in oncomodulin by probing specific sites within the molecule. This was accomplished by an examination of the fluorescence properties of a number of site-specific mutants of oncomodulin in which tryptophan had been selectively placed, and phenylalanine had been substituted in place of the two tyrosine residues. Native oncomodulin possesses two tyrosyl residues in positions 57 and 65 of the 108-residue primary amino acid sequence and no tryptophan. The first two mutations involved the substitution of phenylalanine in place of one tryosyl residue (Y57F[1] and Y65F). Because phenylalanine does not absorb at 280 nm, these mutations allowed the tyrosine fluorescence in each site to be probed individually. As the fluorescence of Trp is more sensitive than Tyr to local interactions and structure, the second set of mutations involved the substitution of Trp for Tyr in positions 57 and 65 (Y57W and Y65W). Further, since the amide carbonyl of Tyr-57 functions as a Ca^{2+}-binding ligand at position 7 in the CD-loop, and Tyr-65 lies just outside of the CD-loop in the flanking D-helix, it was desirable to select a position in the EF-loop for the placement of a Trp probe. Thus, the mutant K96W was prepared as the amide carbonyl of Lys-96 at position 7 in the EF-loop functions as a Ca^{2+}-binding ligand and resides in the analogous position of Tyr-57 in the CD-loop. Figure 1 highlights the positions of the various mutations relative to the two calcium-binding loops. The combination of steady-state and time-resolved fluorescence spectroscopy permitted a detailed assessment of how calcium binding influenced the conformational heterogeneity in the selected regions of the protein structure.

Materials and Methods

Materials

Sodium cacodylate was purchased from Sigma Chemical Co., St. Louis, MO. Potassium chloride was purchased from

† Issued as NRCC Publication No. 31956.

* To whom correspondence should be addressed.

‡ Institute for Biological Sciences, National Research Council.

§ C.M.L.H. is a 1967 NSERC scholar engaged in predoctoral training in the Department of Biochemistry, University of Ottawa, working under the supervision of A.G.S. at the NRC.

‖ Biotechnology Research Institute, National Research Council.

[1] The notation "letter-number-letter" is read as follows: the first letter represents the IUPAC–IUB-established one-letter amino acid code of the native residue, the number identifies the position of the native residue, and hence the position of the point mutation, and the second letter is the code for the amino acid which is being substituted by mutagenesis in place of the native residue.

0006-2960/91/0430-7652$02.50/0 Published 1991 by the American Chemical Society

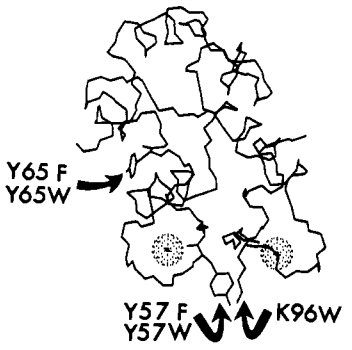

FIGURE 1: X-ray crystallographic structure of oncomodulin highlighting the native residues Tyr-57, Tyr-65, and Lys-96 and the identity of the point mutations at each position. The atomic spheres of the calcium ions are also shown.

Fisher Scientific Co., Ottawa, Ontario, Canada. Trichloroacetic acid (TCA) was obtained from Anachemia, Montreal, Quebec, Canada. L-Tyrosine (99+%) and *N*-acetyltryptophanamide (NATA) were purchased from Aldrich Chemical Co., Milwaukee, WI. The bicinchoninic acid (BCA) protein assay reagent was purchased from Pierce, Rockford, IL. Calcium chloride and magnesium chloride were purchased from Thiokol/Ventron, Danvers, MA. All buffers were prepared by using reverse osmosis quality water purified by the Milli-Q Water System, Millipore Canada Ltd., Mississauga, Ontario, Canada.

Methods

The mutagenesis, plasmid characterization by DNA sequencing, expression, and purification were performed according to the procedures outlined in detail elsewhere (MacManus et al., 1989). In an earlier study, it had been reported, on the basis of tryptic peptide mapping and ^{1}H NMR spectroscopy, that 50–60% of the bacterially expressed protein still retained the initiation amino acid *N*-formylmethionine (MacManus et al., 1989). Although various methods were used to confirm that the recombinant protein, with the heterogeneous N-terminus, folded in an identical manner with the native protein (MacManus et al., 1989), an additional bacterial recombinant oncomodulin known as MAP–BRONCO (methionine aminopeptidase–bacterial recombinant oncomodulin) was produced in the presence study in order to confirm that a heterogeneous N-terminus was not affecting the fluorescence results. MAP–BRONCO, with a homogeneous N-terminal serine residue, was produced in the following way. The 3.1-kb *Eco*RI–*Hin*dIII DNA fragment from pSYC 1174 (Ben-Bassat et al., 1987) containing the *Escherichia coli* methionine aminopeptidase gene was isolated. This DNA fragment was made blunt by treatment with the large fragment of DNA polymerase I (Klenow) and ligated to pGEM. TAC.ONCO which had been linearized with *Pvu*III. *E coli*, transformed with this plasmid, overexpressed both oncomodulin and methionine amino peptidase. The oncomodulin purified from these recombinant bacteria had a homogeneous N-terminus (NH_2-Ser) shown by tryptic peptide mapping, amino acid analysis, and sequencing. Native rat oncomodulin from Morris hepatoma 5123tc was also purified as previously described (MacManus, 1980).

Apoprotein Preparation. The calcium-loaded proteins were decalcified by precipitation with trichloroacetic acid (TCA) (Haiech et al., 1981). This method was found to be satisfactory in achieving greater than 96% decalcification as well as permitting reversible calcium reconstitution (MacManus et al., 1984; Hutnik et al., 1990b). Calcium content following apoprotein preparation was measured by inductively coupled plasma atomic absorption spectrometry. Typically, 0.03–0.08 mol of Ca^{2+}/mol of protein was measured following TCA treatment. The calcium concentration in the buffers prepared by using reverse osmosis quality water was found to be <0.1 μM.

Spectroscopy and Instrumentation. The method of time-correlated single photon counting (TCSPC) was used in the fluorescence decay experiments which, in combination with the steady-state fluorescence data, permitted the construction of decay-associated spectra (DAS). Details of the time-resolved methods and data analysis have been reported earlier (Hutnik & Szabo, 1989; Willis & Szabo, 1989). The emission band-pass was 4 nm. The steady-state fluorescence measurements were performed on an SLM 8000C spectrofluorometer equipped with a Neslab Endocal refrigerated circulating bath for temperature control. All fluorescence emission spectra were corrected as described previously (Hutnik et al., 1990a). Fluorescence quantum yields (ϕ_f) were measured at 20 °C using L-tyrosine (recrystallized 3 times from water prior to use, ϕ_f = 0.135; Chen, 1967) for the Tyr-containing mutants and *N*-acetyltryptophanamide (NATA, ϕ_f = 0.14; Eisinger, 1969) for the Trp-containing mutants as the quantum yield standards. Each standard was dissolved in the same buffer as the protein solutions, pH 7, and was bubbled with nitrogen for 10 min prior to measurement. When the ϕ_f was being measured, the optical density of all solutions at the excitation wavelength was less than 0.10.

The titration data were obtained by the addition of aliquots of either 1 mM $CaCl_2$ or 2 mM $MgCl_2$ with continuous stirring to 1.5 mL of apoprotein. All solutions were prepared in 10 mM cacodylate/150 mM KCl, pH 7. The protein concentrations were 20–40 μM. Protein concentrations were determined by using the Pierce BCA protein assay reagent. Standard curves were generated by using a series of native tumor oncomodulin concentrations, the latter which were estimated by using the molar extinction coefficient ϵ_{276nm} = 3159 M^{-1} cm^{-1} (MacManus & Whitfield, 1983).

Absorption spectra were recorded on a Varian DMS 200 UV–vis spectrophotometer.

RESULTS

Bacterial versus Native Protein. Previous analysis showed that the bacterial recombinant oncomodulin (BRONCO) was identical with the native hepatoma protein in all residues, except that 50–60% of the expressed protein still retained the initiation amino acid *N*-formylmethionine (MacManus et al., 1989). However, the ultraviolet absorption spectra of native tumor oncomodulin, BRONCO, and MAP–BRONCO were identical (data not shown). The corrected steady-state fluorescence emission spectra and quantum yields of fluorescence (ϕ_f) (Table I) of these proteins were also similar, with the spectra of the bacterial proteins being identical with the spectrum of L-tyrosine. Upon decalcification, the ϕ_f of all three proteins decreased from a mean value of 0.053 to a mean value of 0.036 when excited at 280 nm (see Table I). Addition of a 100-fold excess of Ca^{2+} to the apoprotein solutions restored 100% of the fluorescence intensity at λ_{max} = 304 nm. In contrast, addition of a 200-fold excess of Mg^{2+} to the apoprotein solutions restored only 61% of the fluorescence intensity which had been lost upon decalcification (ϕ_f = 0.046). Each of the three apoproteins responded to metal ion titration in a similar manner, with 1 Ca^{2+} equiv restoring greater than 74% of the total fluorescence of the holoprotein. Mg^{2+} titration revealed a much more gradual and noisy response, with plateau fluorescence values occurring only after the addition of 3–4 equiv of Mg^{2+} (data not shown).

Table I: Quantum Yield Summary of the Tyrosine-Containing Oncomodulin Proteins[a]

protein	holo	apo	apo + Ca^{2+}	apo + Mg^{2+}
native oncomodulin	0.052 ± 0.004	0.037 ± 0.003	0.052 ± 0.004	0.046 ± 0.004
BRONCO	0.055 ± 0.003	0.036 ± 0.002	0.054 ± 0.005	0.047 ± 0.003
MAP-BRONCO	0.052 ± 0.003	0.036 ± 0.002	0.052 ± 0.003	0.046 ± 0.003
Y57F	0.016 ± 0.004	0.023 ± 0.003	0.018 ± 0.004	0.023 ± 0.003
Y65F	0.072 ± 0.002	0.041 ± 0.003	0.074 ± 0.003	0.057 ± 0.005

[a] λ_{ex} = 280 nm; 20 °C. All values were obtained relative to L-tyrosine measured under identical conditions. The errors quoted are standard errors of the mean obtained from at least three determinations of the ϕ_f of each sample. The protein concentrations were 20–40 μM, and Ca^{2+}(aq) and Mg^{2+}(aq) were added to a final concentration of 2.5 and 5 mM, respectively.

Table II: Various Steady-State and Time-Resolved Fluorescence Decay Parameters of the Tyrosine-Containing Recombinant Oncomodulin Proteins BRONCO, Y57F, and Y65F (λ_{ex} = 284 nm; λ_{em} = 310 nm; 20 °C)

sample[a]	SVR[b]	σ[b]	τ_1 (ns)	τ_2 (ns)	τ_3 (ns)	α_1[c]	α_2[c]	α_3[c]	$\langle\tau\rangle$[d] (ns)
holo-BRONCO	2.00	1.04	3.19 ± 0.02	1.04 ± 0.05	0.322 ± 0.015	0.33	0.30	0.37	1.48
apo-BRONCO	1.96	1.05	2.87 ± 0.03	1.13 ● 0.04	0.289 ± 0.011	0.24	0.34	0.42	1.19
holo-Y57F	1.89	1.14	2.95 ± 0.06	0.81 ± 0.03	0.278 ± 0.010	0.06	0.38	0.56	0.64
apo-Y57F	1.85	0.99	2.07 ± 0.03	0.85 ± 0.04	0.245 ± 0.007	0.16	0.28	0.56	0.71
holo-Y65F	1.99	1.02	3.22 ± 0.02	1.58 ± 0.05	0.058 ± 0.009	0.46	0.22	0.32	1.85
apo-Y65F	1.92	1.01	2.90 ± 0.02	1.11 ± 0.06	0.267 ● 0.011	0.29	0.25	0.46	1.24

[a] All protein samples were in 10 mM cacodylate/150 mM KCl, pH 7.0. In addition, 1 mM $CaCl_2$ was added to the holo samples to ensure complete occupancy of the metal-binding sites. [b] SVR represents the serial variance ratio and, σ is defined as the square root of the reduced χ^2 (χ_r^2). SVR and σ are statistical parameters reflecting the goodness of fit. "Ideal" statistical fits correspond to an SVR = 2 and σ = 1 [see McKinnon et al. (1977)]. [c] α_i denotes the normalized preexponential term of the ith decay time component. The α_is are the same as the relative ground-state component concentrations assuming that the radiative lifetime of each component is the same and static quenching is absent (Donzel et al., 1974; Hutnik & Szabo, 1989). [d] $\langle\tau\rangle$ is the mean (defined in eq 1).

Tyrosine-Containing Mutant Proteins. The substitution of Phe into the place of each tyrosyl residue (Y57F, Y65F) allowed the fluorescence response of each tyrosine to be examined independently. The absorption spectra of the holo mutant proteins both showed increased intensity of the structured Phe bands in the region of 260–280 nm relative to the intensity of the Tyr absorption maximum at 280 nm. The corrected steady-state fluorescence emission spectra of both the holo and apo mutant proteins had λ_{max} in the identical position as BRONCO (λ_{max} = 304 nm). Decalcification of Y65F resulted in a decrease in the fluorescence intensity whereas the spectrum of Y57F experienced an increase in fluorescence intensity at 304 nm (Figure 2). The ϕ_f of Y65F (0.072) was approximately 5 times greater than the ϕ_f for Y57F (0.016) (see Table I).

Ca^{2+} titration of apo-Y65F produced changes in the fluorescence emission spectrum (λ_{ex} = 280 nm; λ_{em} = 306 nm) which differed from that of BRONCO (Figure 3). A greater percentage of the fluorescence change was complete after addition of 1 equiv of Ca^{2+} to BRONCO (74%) when compared to Y65F (53%). Fifty percent of the maximum fluorescence response was complete upon the addition of 0.5 Ca^{2+} equiv to BRONCO; this contrasts with the 1 Ca^{2+} equiv that was required to produce 50% of the maximum fluorescence response for Y65F. The fluorescence intensity changes upon Mg^{2+} titration of Y65F did not plateau, even after addition of 4 metal ion equiv. The titration curves of Y57F were similar in shape to Y65F but were considerably more noisy owing to its weak fluorescence (data not shown).

Time-resolved fluorescence measurements indicated that all of the tyrosine-containing proteins were best fit by triple-exponential decay functions either in the presence or in the absence of Ca^{2+}. In Table II, the fluorescence decay parameters obtained at λ_{ex} = 284 nm and λ_{em} = 310 nm are shown, together with the mean lifetime. The mean lifetime ($\langle\tau\rangle$) was calculated according to the relationship:

$$\langle\tau\rangle = \sum\alpha_i\beta_i \quad (1)$$

where the α_i's are the preexponential terms which are pro-

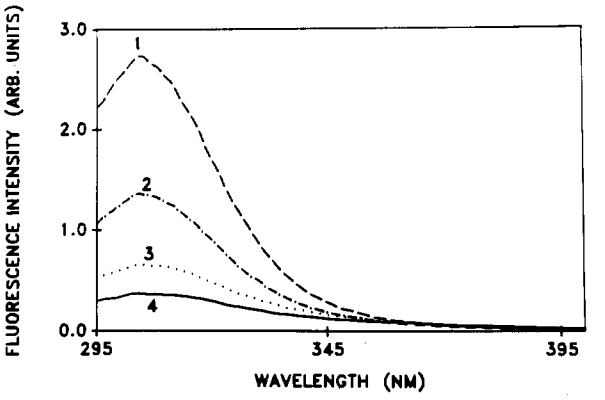

FIGURE 2: Corrected steady-state fluorescence emission spectra of Y57F and Y65F oncomodulin mutant proteins in the absence (apo) and presence (holo) of Ca^{2+}. (1) Dashed line, holo-Y65F; (2) dashed–dotted line, apo-Y65F; (3) dotted line, apo-Y57F; (4) solid line, holo-Y57F. The protein concentrations were approximately 25 μM, λ_{ex} = 280 nm, excitation and emission band-pass = 4 nm, 20 °C.

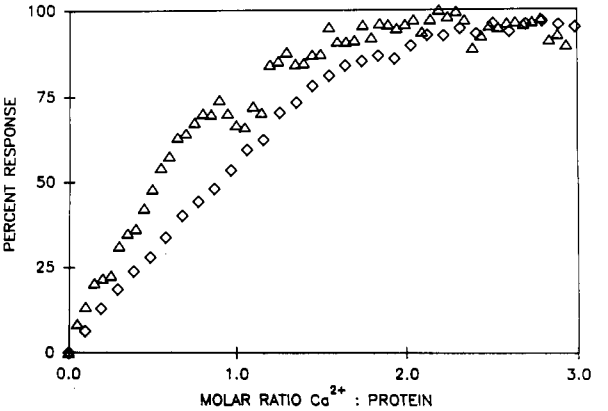

FIGURE 3: Ca^{2+} titration curves of apo bacterial recombinant oncomodulin (BRONCO, △) and Y65F oncomodulin mutant protein (◇) plotted in terms of the fluorescence intensity change upon Ca^{2+} addition. λ_{ex} = 280 nm; λ_{em} = 306 nm, 20 °C.

portional to the fractional concentration of each component and the β_i's are the individual decay time components. The lifetime values of Y65F more closely resembled those of BRONCO when compared to the values of Y57F. The mean lifetime, $\langle\tau\rangle$, of Y65F decreased by approximately 33% upon decalcification, whereas the ϕ_f decreased to a greater degree (43%). The fluorescence parameters of Y57F were significantly different when compared to the other two proteins. Instead of quenching, decalcification induced an enhancement of the tyrosine fluorescence (Table I). The ϕ_f increased from 0.015 to 0.023 upon decalcification, which was reflected in the increase in α_1 from 0.06 to 0.16 (Table II) despite only a 11% increase in the mean lifetime. The lifetime values of the longest and middle decay components were significantly less both in the presence and in the absence of Ca^{2+} when compared to BRONCO and V65F.

Tryptophan-Containing Mutant Proteins. The absorption spectra of Y57W, Y65W, and K96W were similar both in the absence and in the presence of Ca^{2+} (data not shown) and, in each case, lacked a sharp 292-nm subsidiary peak as was observed in cod III parvalbumin and another oncomodulin mutant, F102W (Hutnik et al., 1990a).

Selective excitation of the single Trp residues at 295 nm showed that only Trp in position 57 was perturbed to a significant extent upon decalcification (Figure 4A). A significant variation of ϕ_f in the three mutant proteins was observed depending upon the position of the tryptophan. The ϕ_f of Y57W increased from 0.078 to 0.133 upon Ca^{2+} removal. For Y65W and K96W, decalcification resulted in only a slight decrease in the tryptophan fluorescence emission, the ϕ_f of Y65W decreasing from 0.157 to 0.143 and the ϕ_f of K96W decreasing from 0.084 to 0.079. The λ_{max} values of the emission spectra of apo-Y65W and apo-K96W were slightly blue-shifted by 3–4 nm relative to each respective holoprotein, while, in contrast, no change was observed in the wavelength position of the emission maximum of either form of Y57W. In all cases, addition of Ca^{2+} to the apoproteins restored 100% of the fluorescence intensity, while Mg^{2+} addition had only a minor influence when compared to the intensity of the apoprotein (shown for Y57W in Figure 4A).

Upon excitation of both Tyr-65 and Trp-57 in Y57W at 280 nm, similar fluorescence intensity changes on going from the apo to metal-bound forms were obtained when compared to the 295-nm excited spectrum. No significant shoulder at 304 nm that could be assigned to tyrosine on excitation at 280 nm was evident. However, when Y65W was excited at 280 nm, intensity changes at 304 nm were observed which depended on the metal content. No changes at this emission wavelength were seen when this mutant was excited at 295 nm. At both excitation wavelengths, minor changes were observed at 350 nm (Figure 4B). The metal-dependent changes at 304 nm on excitation at 280 nm must be the result of excitation of Tyr-57 in Y65W. These intensity changes, albeit small in an absolute sense, were in the same proportion as those metal-dependent intensity changes observed for the BRONCO protein.

The fluorescence emission spectra of K96W, when excited at 280 nm where Tyr-57 and Tyr-65 were also excited, were different when compared to the same protein excited at 295 nm (only Trp-96 was excited). Compared to the 6% decrease in fluorescence intensity upon decalcification at λ_{ex} = 295 nm, an 18% decrease was observed when λ_{ex} = 280 nm (Figure 4C). While Ca^{2+} addition to K96W restored 100% of the fluorescence intensity, Mg^{2+} addition restored only 44% of the fluorescence intensity which had been lost upon Ca^{2+} removal (λ_{ex} = 280 nm). The fluorescence excitation spectrum (Figure

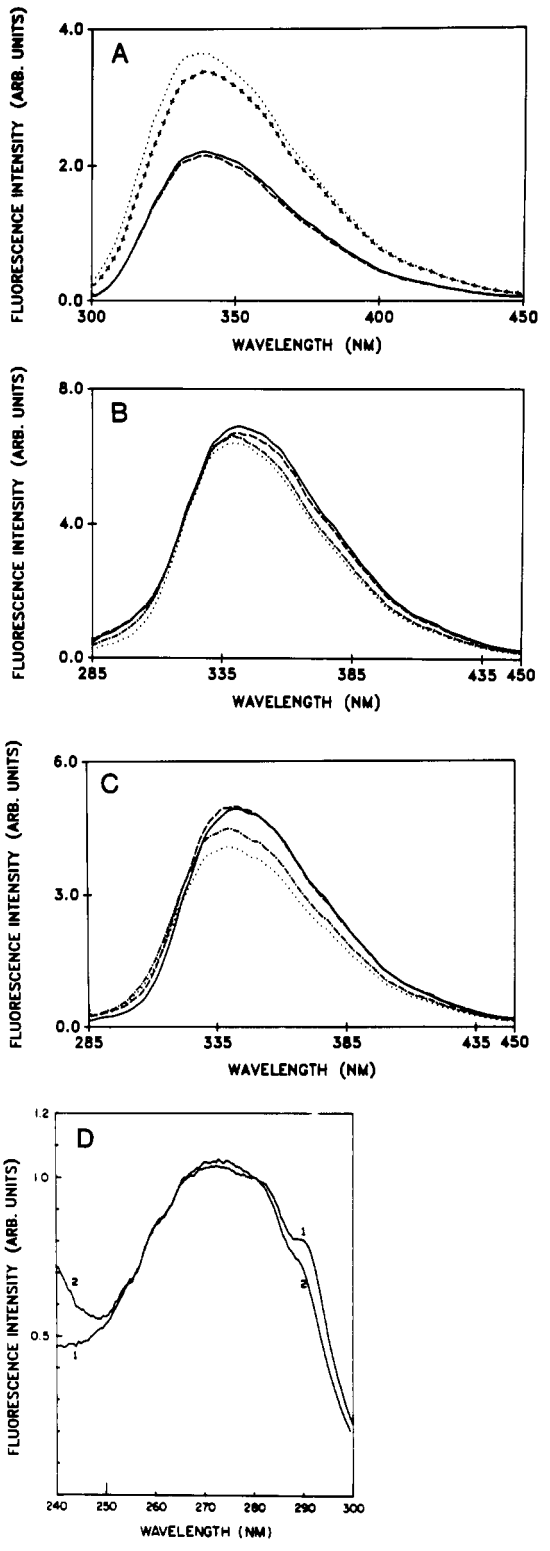

FIGURE 4: Corrected steady-state emission spectra of (A) Y57W, λ_{ex} = 295 nm; (B) Y65W, λ_{ex} = 280 nm; and (C) K96W, λ_{ex} = 280 nm, showing the response of the proteins to Ca^{2+} and Mg^{2+} addition. The protein concentration was approximately 25 μM. $CaCl_2$ was added to a final concentration of 2.5 mM, an $MgCl_2$ was added to a final concentration of 5 mM. Excitation and emission band pass = 4 nm, 20 °C. In (A), (1) dotted line, apo-Y57W; (2) short-dashed line, apo-Y57W + Mg^{2+}; (3) solid line, holo-Y57W; (4) long-dashed line, apo-Y57W + Ca^{2+}. In (B), solid line, holo-Y65W; dotted line, apo-Y65W; dashed line, apo-Y65W + Ca^{2+}; dashed–dotted line, apo-Y65W + Mg^{2+}. In (C), solid line, holo-K96W; dotted line, apo-K96W; dashed line, apo-K96W + Ca^{2+}; dashed–dotted line, apo-K96W + Mg^{2+}. In (D), the fluorescence excitation spectra of (1) holo-Y65W and (2) holo-K96W are shown, excitation and emission band-pass = 4 nm, 20 °C, λ_{em} = 305 nm.

Table III: Various Steady-State and Time-Resolved Fluorescence Decay Parameters of the Tryptophan-Containing Oncomodulin Mutants Y57W, Y65W, and K96W (λ_{ex} = 295 nm; 20 °C)

sample[a]	ϕ_f	λ^{ss}_{max}[b] (nm)	SVR[c]	τ_1[d] (ns)	τ_2 (ns)	τ_3 (ns)	λ^1_{max}[e] (nm)	λ^2_{max} (nm)	λ^3_{max} (nm)	F_1[f]	F_2	F_3	c_1[f]	c_2	c_3	τ_r[g] (ns)	$\langle\tau\rangle$[h] (ns)
holo-Y57W	0.078 ± 0.003	339	1.98	6.17 ± 0.02	1.61 ± 0.01	0.374 ± 0.015	345	338	330	0.29	0.67	0.04	0.09	0.75	0.17	23.4	1.83
apo-Y57W	0.133 ± 0.003	340	1.98	5.25 ± 0.01	2.05 ± 0.02	0.504 ± 0.009	344	331	330	0.51	0.44	0.05	0.24	0.51	0.25	18.3	2.43
holo-Y65W	0.157 ± 0.003	343	1.90	5.13 ± 0.01	1.97 ± 0.01	0.167 ± 0.005	349	338	338	0.54	0.44	0.02	0.25	0.51	0.24	14.8	2.33
apo-Y65W	0.143 ± 0.002	340	1.89	4.05 ± 0.01	2.03 ± 0.01	0.213 ± 0.006	344	336	337	0.57	0.41	0.02	0.32	0.47	0.21	16.1	2.29
holo-K96W	0.084 ± 0.004	342	1.94	5.85 ± 0.02	2.30 ± 0.04	0.133 ± 0.003	347	332	340	0.84	0.15	0.02	0.41	0.18	0.41	34.0	2.86
apo-K96W	0.079 ± 0.003	339	1.89	5.06 ± 0.02	1.95 ± 0.02	0.373 ± 0.006	339	332	332	0.63	0.32	0.05	0.29	0.39	0.32	29.7	2.35

[a] All protein samples were in 10 mM cacodylate/150 mM KCl, pH 7.0. In addition, 1 mM $CaCl_2$ was added to the holo samples to ensure complete occupancy of the metal-binding sites. The protein concentration was 20–40 μM. [b] λ^{ss}_{max} represents the wavelength of maximum intensity in the corrected steady-state fluorescence emission spectrum. [c] SVR represents the serial variance ratio. It is a statistical parameter reflecting the goodness of fit. An SVR = 2 corresponds to an ideal statistical fit of the data (McKinnon et al., 1977). The SVR values shown reflect the statistics obtained upon global analysis of 10 data sets. [d] The errors quoted for the lifetime values represent the standard errors for lifetime recovery from a given global set. [e] λ^i_{max} represents the wavelength of the maximum intensity emission of the various components whene excited at 295 nm. These values are obtained from the DAS. [f] F_i and c_i denote the fractional fluorescence and relative concentrations, respectively, of the various decay time components at 320 nm. The c_is were equivalent to the normalized preexponential terms. [g] τ_r represents the radiative lifetime and was calculated by assuming that it was the same for all of the decay components in a given protein sample. [h] $\langle\tau\rangle$ is the mean lifetime.

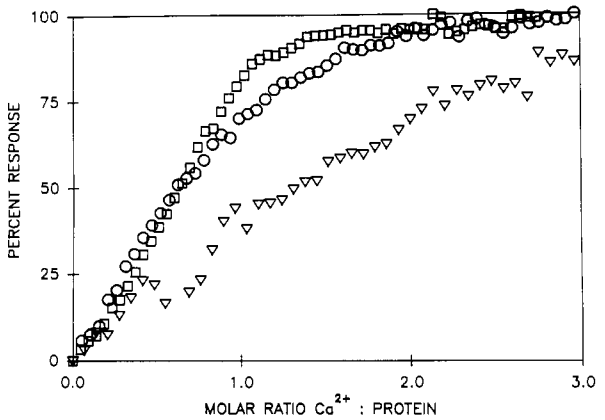

FIGURE 5: Ca^{2+} titration of apo-Y57W (□), Y65W (○), and K96W (△) plotted in terms of the fluorescence intensity changes at the excitation and emission wavelengths of maximum fluorescence response. For Y57W, λ_{ex} = 295 nm, λ_{em} = 350 nm; for Y65W, λ_{ex} = 280 nm, λ_{em} = 300 nm; for K96W, λ_{ex} = 280 nm, λ_{em} = 350 nm.

4D, λ_{em} = 305 nm) of K96W possessed a greater tyrosine component compared to the fluorescence excitation spectrum of Y65W.

Ca^{2+} titration revealed that the various apoproteins experienced different fractional changes in the fluorescence at various substoichiometric amounts of Ca^{2+}. In Figure 5, the Ca^{2+} titration curves for the three Trp-containing mutant proteins obtained at wavelengths of maximal fluorescence response are shown. Upon comparison, 1 Ca^{2+} equiv had the greater influence on the fluorescence response of Y57W (squares), followed by Y65W (circles) and, lastly, by K96W (triangles). One equivalent of Ca^{2+} produced greater than 70% of the maximal fluorescence response in Y57W and Y65W, whereas the same amount of Ca^{2+} produced only 41% of the maximal fluorescence response in K96W.

Time-resolved fluorescence of the three Trp-containing oncomodulin mutant proteins showed that the fluorescence decay of the holo- and apoproteins obeyed triple-exponential decay kinetics. The various fluorescence parameters are summarized in Table III. The longest lived decay component, τ_1, ranged between 5 and 6 ns, while the middle decay component, τ_2, ranged between 1.6 and 2.3 ns and the shortest lived decay component, τ_3, had a value ranging between 0.1 and 0.5 ns.

In holo-Y57W, the middle decay component (τ_2 = 1.61 ns) had both the greatest contribution to the total fluorescence (Figure 6A) and also the greatest component concentration (75%). Decalcification resulted in a decrease in the fractional contribution of this component to the fluorescence, a substantial blue-shift in the DAS of this component from 338 nm (holo) to 331 nm (apo), and a decrease in the relative component concentration to 51% (Figure 6B). The λ_{max} of the short-lifetime component in both holo- and apo-Y57W occurred at 330 nm. Given that $\phi_f = \tau_s/\tau_r$, where τ_s and τ_r are the singlet and radiative lieftimes, respectively, upon decalcification the 33% increase in the mean lifetime $\langle\tau\rangle$ did not parallel the 71% increase in ϕ_f. Assuming that the τ_r for each lifetime component is the same in a given protein and static quenching is absent (Donzel et al., 1974), it is possible to calculate the value of τ_r by using the equation:

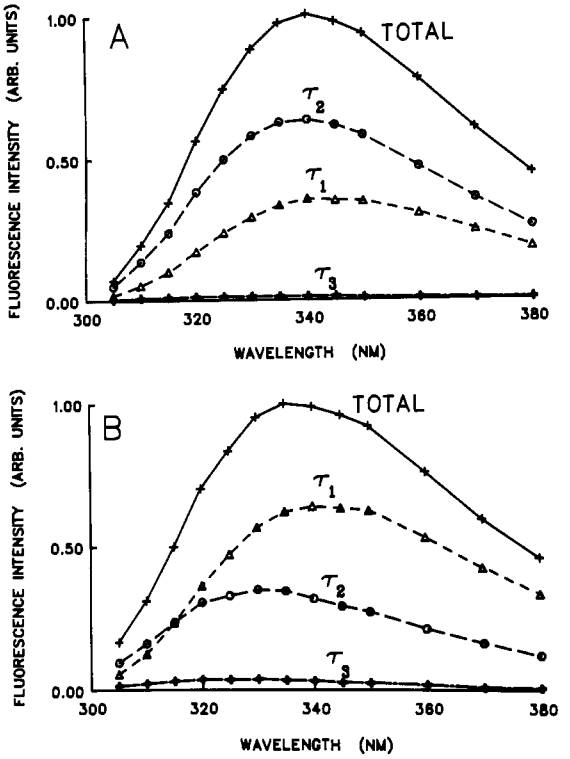

FIGURE 6: Decay-associated spectra for (A) holo-Y57W and (B) apo-Y57W oncomodulin mutant protein. The spectra sum to the corresponding corrected steady-state spectral intensities normalized to a value of 1 unit at the emission maximum. Standard errors are within the contours of the plotted symbols.

$$\phi_f = \sum(c_1\tau_1 + c_2\tau_2 + c_3\tau_3)/\tau_r \quad (2)$$

where ϕ_f is the total quantum yield of fluorescence, c_i is the relative concentration of the ith component [c_i is equivalent to α_i if it is assumed that τ_r is the same for each component; see Hutnik and Szabo (1989) for elaboration], and τ_i is the straight lifetime of the ith component. When this is done, τ_r = 23 ns for holo-Y57W and τ_r = 18 ns for apo-Y57W.

In Y65W, the longest lived decay component dominated the fluorescence emission both in the absence and in the presence

of Ca^{2+}, despite the relatively larger concentration of the middle lifetime component (Table III). The λ_{max} of the longest decay component occurred at a relatively long wavelength position of 334–349 nm, which contrasted the blue-shifted emission of both the middle and shortest decay components (336–338 nm) both in the absence and in the presence of Ca^{2+}. Decalcification did not alter either the fractional fluorescences, the relative component concentrations, or the DAS to any great extent in Y65W (Table III). The mean lifetime decreased by 2% from 2.33 to 2.29 ns upon Ca^{2+} removal and corresponds well with the 9% decrease in ϕ_f. Calculation of the τ_r values showed that decalcification had virtually no effect upon this parameter (Table III).

Although the ϕ_f of K96W decreased by only 6% upon decalcification, an 18% decrease in the mean lifetime was observed. In addition, the DAS of the longest and shortest decay components experienced substantial blue-shifts upon decalcification [λ_{max}^1(holo–K96W) = 347 nm vs λ_{max}^1(apo-K96W) = 339 nm; λ_{max}^3(holo-K96W) = 340 nm vs λ_{max}^3(apo-K96W) = 332 nm]. The middle decay time component had both a greater fractional fluorescence and a component concentration upon decalcification, and there was no change in the position of λ_{max} of the DAS of this component (Table III). The radiative lifetime of holo-K96W (34 ns) was considerably longer than that of the other proteins (Y57W and Y65W) and decreased upon decalcification to 30 ns.

Discussion

Bacterial versus Native Protein. The absorption spectra, fluorescence emission spectra, and quantum yields of fluorescence of the bacterial recombinant oncomodulin (BRONCO) were identical with the native tumor protein. In addition, both apoproteins responded to metal ion titration in an identical manner. Spectral comparison of BRONCO with another bacterially expressed oncomodulin, MAP–BRONCO, further confirmed that the heterogeneous amino terminus did not influence the spectrally determined metal ion binding properties of the protein.

The fluorescence emission spectra of the bacterially expressed tyrosine proteins BRONCO, Y57F, and Y65F showed no evidence of any spectral features on the low-energy side of the spectrum. Previously, a shoulder near 345 nm had been noted in native tumor oncomodulin and was assigned to tyrosinate fluorescence (MacManus et al., 1984). This observation causes us to conclude that the previous appearance of the shoulder was most likely due to the presence of a small amount of a Trp-containing contaminant, rather than excited-state formation of tyrosinate anion.

On the basis of the titration data and the ϕ_f's, it is clear that Mg^{2+} binding to oncomodulin does not have the same effect as Ca^{2+} on the conformation response of oncomodulin. These are obviously some specific Ca^{2+}-induced structural changes. Similar results were reported for ram testis and octopus calmodulins, where it was found that, at physiological ionic strength (150 mM KCl), Mg^{2+} binding did not exert a major influence on protein conformation (Kilhoffer et al., 1981).

Tyrosine-Containing Mutant Proteins. The replacement of each tyrosine residue by phenylalanine permitted an assignment of the origin of the fluorescence changes observed in the native protein. The impact of metal ion binding on the environment associated with each site (positions 57 and 65) was revealed.

A low ϕ_f (0.016) was measured for Y57F. Inspection of the crystal structure did not suggest any structural feature or any local interactions of the sole remaining Tyr-65 which might lead to this low ϕ_f. Decalcification of Y57F resulted in a small *increase* in the ϕ_f of Tyr-65 (0.023), indicating that Ca^{2+} binding promotes a small conformational change in the region of Tyr-65 which slightly modifies the quenching process.

In contrast, the effect of decalcification on the ϕ_f of Y65F was opposite to that of Y57F, with the ϕ_f *decreasing* upon Ca^{2+} removal (from 0.072 to 0.041). As the acidic residues in both the CD- and EF-binding loops would no longer be bound to Ca^{2+} upon decalcification, the carboxylate groups of the acidic residues in these loops would now be available for interaction with Tyr-57. The crystal structure shows that Tyr-57 is located close to the EF-binding site. The formation of hydrogen bonds involving Tyr-57 and the acidic residues in the EF-loop in apo-Y65F would explain the observed decrease in ϕ_f. It could be due to proton abstraction from the tyrosine hydroxyl by one of the carboxylate groups (Willis & Szabo, 1990). As Tyr-57 was much more fluorescent than Tyr-65 in both the absence and the presence of Ca^{2+}, the fluorescence of Tyr-57 dominates the intrinsic fluorescence properties of the native protein. The mean ϕ_f of Y57F and Y65F was 0.044, which is 21% less than the 0.055 value for BRONCO. This discrepancy may be due to different absorbancies for the two tyrosine residues at 280 nm, owing to hydrogen bonding to the acidic residues by Tyr-57, or some interaction between the residues in the native protein.

The fluorescence decay parameters of Y65F were similar to those of BRONCO, except that in holo-Y65F the short decay time component (τ_3 = 0.058 ns) is considerably different from the corresponding decay component in holo-BRONCO (τ_3 = 0.322 ns). One can speculate as to the origin of the interaction which leads to such a strong quenching process, but it is felt that no definite assignment can be made. In both proteins, the decrease in ϕ_f upon decalcification was greater than the decrease in the average decay time. This may be due to static quenching or perhaps to changes in the radiative lifetime of the tyrosine residue as considered below for the tryptophan mutants. The correlation of a static quenching process with a structural element of the protein is not obvious. The significantly shorter decay times of Tyr-65 in Y57F require that the environment of Tyr-65 is different from that of Tyr-57 both in the presence and in the absence of Ca^{2+}. Although these tyrosine residues are only separated by eight amino acids, the crystal structure shows that their orientation and position relative to the Ca^{2+}-binding loops are different. Furthermore, the results demonstrate that the most important structural effects of decalcification are localized in the region probed by Tyr-57.

Tryptophan-Containing Mutant Proteins. The absorption spectra of all three Trp-containing mutants lacked a sharp 292-nm subsidiary peak, which was the first indication that the tryptophan residues in the three locations resided in relatively polar environments (Andrews & Forster, 1972). Decalcification did not alter this feature to any significant degree. This contrasts with the holo-F102W mutant where the tryptophan absorption spectrum had a sharp peak at 292 nm (Hutnik et al., 1990a).

The steady-state fluorescence emission spectra of all the Trp-containing mutants had emission maxima in the range of 339–343 nm, both in the absence and in the presence of Ca^{2+} (Figure 4). Only in Y65W and K96W was the fluorescence maximum affected by removal of Ca^{2+}, with a small shift of 3–4 nm to lower wavelength, indicating that the environments of Trp-65 and Trp-96 have become slightly less polar. These observations are consistent with the tryptophan in all these proteins residing in polar, solvent-accessible environments (Van Durren, 1961).

Whereas the efficiency of Trp-57 emission was significantly affected by decalcification, only minor changes were found for either Trp-65 or Trp-96 when excited at 295 nm. The results obtained with Y65W paralleled those found in Y57F, namely, that position 65 did not appear to be much affected by Ca^{2+} binding. The marked increased ϕ_f for Trp-57 on decalcification contrasts with the significant decrease in ϕ_f for Trp-102 reported earlier in the work on the F102W mutant (Hutnik et al., 1990). Clearly, the nature of the environment and the effect of electronic or electrostatic interactions on the tryptophan residues in these different locations are substantially different.

When Y65W was excited at 280 nm, it was the only mutant to display any evidence of tyrosine fluorescence at 304 nm (Figure 4B) arising from Tyr-57. The changes of the tyrosine emission in Y65W produced by decalcification and subsequent Ca^{2+} and Mg^{2+} addition suggesting that the environment of Tyr-57 was behaving in a similar manner as in the native protein and that the substitution of the bulkier tryptophan residue (compared to phenylalanine) (Zamyatnin, 1972) in position 65 did not affect the interactions of Tyr-57. The observation of Tyr-57 fluorescence with 280-nm excitation in this mutant also indicates that resonance energy transfer to Trp-65 may not be occurring to any significant degree (see below). On the other hand, upon excitation at 280 nm, Y57W showed no evidence of any tyrosine fluorescence from Tyr-65, probably because of its significantly lower fluorescence efficiency.

Mutant K96W was the only one in which the relative changes in intensity of the tryptophan fluorescence of the holo and apo forms was dependent on excitation wavelength. With excitation at 295 nm, a small 6% decrease in fluorescence intensity was observed going from the holo to the apo form. With exitation at 280 nm, an 18% decrease was found. This can only be rationalized by the occurrence of resonance energy transfer from Tyr-57 to Trp-96. The tyrosine-like fluorescence excitation spectrum (λ_{em} = 350 nm) of holo-K96W in Figure 4D is further indication of tyrosine to tryptophan energy transfer. The crystal structure shows that Tyr-57 and Trp-96, although located in two separate binding loops, lie in close proximity to each other (Figure 1). The change in resonance energy-transfer efficiency on decalcification requires that Ca^{2+} binding results in a change in the relative orientation of Tyr-57 and Trp-96, which further implies a Ca^{2+}-promoted change in the position of the CD-loop relative to the EF-loop. This resonance energy-transfer behavior in K96W contrasts with the observations seen for Y65W as described above. In this latter mutant, the relative separation and orientation of Tyr-57 and Trp-65 must be such that resonance energy transfer from tyrosine to tryptophan is not favored.

The effect of resonance energy transfer in K96W was highlighted on examination of the Ca^{2+} titration curves at the two different excitation wavelengths. When Trp-96 was directly excited at 295 nm (λ_{em} = 350 nm), 72% of the total fluorescence response was complete upon addition of 1 Ca^{2+} equiv. In contrast, as seen in Figure 5, when the emission of Trp-96 was measured after exciting both tyrosine and tryptophan at 280 nm (λ_{em} = 350 nm), only 41% of the total response was observed upon addition of 1 Ca^{2+} equiv. This is considerably different from the results obtained upon titration of either Y57W or Y65W (Figure 5), where addition of 1 Ca^{2+} equiv promoted greater than 82% of the total fluorescence change in Y57W and greater than 70% change in Y65W. Further monitoring the Tyr-57 emission or the Trp-65 emission in Y65W produced identical titration curves. The effect of excitation wavelength on the metal-dependent fluorescence changes and the 280-nm excitation titration data or the K96W mutant when taken together provide an indication of the relative effects of the binding of Ca^{2+} into the two binding loops and the effect of filling each loop on the conformational properties of oncomodulin. The filling of the higher affinity EF-site (Hapak et al., 1989; Cox et al., 1990) produces important protein conformational structural changes while the second Ca^{2+} equivalent which binds to the CD-loop has an effect of altering the position of the two loops relative to one another.

The fluorescence decay behavior provided additional insights into the local interactions and structural effects of Ca^{2+} binding. Each of the three tryptophan-containing mutants was described by a triple-exponential decay function (Table III). Such multiexponential decay behavior is often observed for tryptophan in proteins, even those containing a single tryptophan residue. It has been rationalized as indicating conformational heterogeneity of the tryptophan residue or protein segment containing the tryptophan (Szabo, 1990).

Each of the holoproteins had three different decay time values. Further, the decay times for the holo and apo forms of each mutant were not the same. The assignment of a decay time value to a particular conformational structure of the protein in the region of the tryptophan is not possible at the present time. Only when correlations of fluorescence decay parameters with protein structural features has been established through studies of several proteins and their mutants may such an assignment be possible. This problem of assignment of decay times is evident when two examples from this work are considered, namely, holo-Y57W and apo-K96W. The quantum yields of these mutants are the same, but the decay times and the fractional fluorescence values are significantly different.

By combining the steady-state and time-resolved fluorescence data, it was possible to construct decay-associated spectra (DAS) of each of the decay components. The DAS provide information on the environment of the different conformational states indicated by the multiexponential decay, as well as on the relative amounts of each component (Knutson et al., 1982). The spectral maximum of the DAS of the long decay time component in each mutant in both the holo and the apo forms appeared at relatively long wavelength, >344 nm (except for apo-K96W, 339 nm). This indicates that the conformational component with the long decay time is in a polar environment. The spectral maximum of the middle decay time component is always found at shorter wavelength and in the case of Y57W is significantly affected by Ca^{2+}. The very low fluorescence contribution of the short decay time component makes it difficult to locate its spectral maximum with any degree of certainty.

Consistent with the steady-state fluorescence data, the time-resolved fluorescence parameters of Y57W were significantly affected by the presence or absence of Ca^{2+}, indicating that the structure and interactions of Trp-57 were different in the holo and apo forms. The long lifetime component changed from 6.17 to 5.25 ns, the middle decay time changed from 1.61 to 2.05 ns, and the short decay time component changed from 0.374 to 0.504 ns going from the holo- to apoprotein. The decrease in the value of the long decay time component did not parallel the marked increase in ϕ_f; however, the relative amount of this component increased from 0.09 to 0.24, thus partially compensating for the decreased lifetime value. The mean decay time increased by 33%, but this was not consistent with the 71% increase in ϕ_f. The spectral

position of the DAS of the middle decay time component shifted to higher energy by 7 nm in the apo form, the largest change seen in any component in all the mutants studied. This indicates that the environment of the tryptophan in the conformation represented by that decay time became relatively less polar on removal of the Ca^{2+}.

In the case of Y65W, only the long decay time component changed on going from the holo to the apo form, decreasing from 5.13 to 4.05 ns. The change in the relative concentration of this component, however, increased, resulting in no change in the mean lifetime nor in the ϕ_f on loss of Ca^{2+}. Hence, while the spectra and ϕ_f appeared not to be affected by decalcification, the decay time parameters indicated that a structural change occurred which affected the interactions of one of the tryptophan conformers in this mutant, albeit much less than in the Y57W mutant. Crystal structure parameters show that the α-carbon of residue 65 is 11 Å away from the Ca^{2+} in the CD-loop and 19 Å away from the EF-loop. The same distances for α-carbon 57 are 4.5 and 8.0 Å, respectively.

The decay parameters obtained for K96W further confirm that the Ca^{2+}-induced conformational changes are more pronounced in the region of the metal-binding loops. Not only were the three decay times different in the holo and apo forms but also the fractional composition of the three components changed. The spectral maxima of the DAS of both the long and short decay time components were blue-shifted by 8 nm in the apo form. While the ϕ_f was hardly affected, the mean decay time decreased by 25% in the apoprotein. These results indicate that the interactions and the electronic environment of Trp-96 were significantly altered on decalcification.

The lack of correlation of ϕ_f with the fluorescence decay times measured for the different proteins, for example, comparing holo-Y65W ($\phi_f = 0.157$; decay times of 5.13, 1.97, and 0.167 ns; mean decay time of 2.33 ns) and holo-Y57W ($\phi_f = 0.078$; decay times of 6.17, 1.61, and 0.374 ns; mean decay time of 1.83 ns), and the lack of correspondence of the ϕ_f and mean decay time of the holo and apo forms of each mutant require comment. A rationalization which is often suggested is that there must be some static quenching occurring. Inspection of the crystal structure does not reveal any features which might lead to a static quenching process. However, the presence or absence of Ca^{2+} should markedly affect the electronic environment of the tryptophan residues, especially when the amide carbonyl group of the tryptophan is one of the ligands of the metal in the binding site. In the case of the blue copper proten azurin, it was suggested that the radiative lifetime of the single tryptophan residue was affected by the presence or absence of the Cu^{2+} ligand (Hutnik & Szabo, 1989). This was also suggested to be the case in cod parvalbumin and oncomodulin mutant F102W (Hutnik et al., 1990). In a recent paper, it was shown that the single tryptophan residue in phosphoglycerate mutase had a very long decay time of 16.4 ns and that its τ_r was 53 ns (Schauerte & Gafni, 1989), which is much greater than the value of 23 ns which is usually taken as the τ_r for tryptophan in proteins. It is proposed that in the oncomodulin mutant proteins the radiative lifetime, τ_r, depends on the location of the tryptophan residue and its local electronic environment. When τ_r was calculated (Table III) for Y57W, the value for the holoprotein was 23.4 ns, while it was 18.3 ns for the apo form, a change of 5 ns! The presence or absence of bound Ca^{2+} would certainly affect the local electrostatic interactions of Trp-57. By contrast, in Y65W, τ_r was hardly affected. The calculated values of τ_r for K96W were 34 and 29.7 ns for the holo and apo forms, respectively. These values are considerably longer than those calculated for other mutants and approach that estimated for phosphoglycerate mutase. They must reflect a special electronic environment for the tryptophan residue in this K96W mutant.

The discussion of Schauerte and Gafni provides a useful consideration of the various alternatives which could lead to such a variation of the value of τ_r. Particularly relevant to the data reported in this work is their suggestion that static charge perturbations will perturb the electronic transition moments of the lowest excited singlet states of the chromophore. This perturbation could distort the geometry of the charge-transfer state of the indole ring following excitation and stabilize the excited state, therefore affecting radiative lifetime. Also relevant to this rationalization is the work of Ilich and co-workers (Ilich et al., 1988), who performed quantum-mechanical calculations on the effect of static charge on the electronic transitions of indole and Trp-59 in ribonuclease T_1. Their work demonstrated that the spectra and transition intensities were influenced by static charge and the direction of the charge field. Again, in model compound studies on indoles, it was shown that τ_r was affected by the polarity of the environment (Privat et al., 1979).

It follows from the above rationalization that tryptophan in positions 57 and 96, while occupying analogous positions as binding ligands in the two binding loops, experiences different electronic field environments. Each of these tryptophan residues is affected by the binding of Ca^{2+}, with the fluorescence response of Trp-57 being significantly greater than that of Trp-96. The majority of the fluorescence intensity change for Trp-57 originates when the charge of the EF-loop is changed by the binding of Ca^{2+}.

Conclusion

This study has demonstrated how the variation of fluorescence properties of tryptophan and tyrosine in different locations in oncomodulin has provided new insights into the structural features which are affected by Ca^{2+} binding. First, the results show that the protein retains its overall structural integrity even in its apo form. Further, the fluorescence properties of the Ca^{2+}-reconstituted forms are virtually identical with those of the holoprotein. It therefore follows that the structure of the reconstituted protein is the same as the native, Ca^{2+}-loaded, structure. It is proposed that binding to the EF-loop results in important secondary structural changes in the region of the binding loops, essentially locking the protein into its native conformation. Binding of the second equivalent of Ca^{2+} to the CD-loop results in only a subtle change in orientation of the CD-loop relative to the EF loop. This would be consistent with the CD-loop being the loop responsible for oncomodulin's modulatory activity. Such small structural changes would minimize entropy changes and hence render its modulatory activity more efficient.

The data presented on these mutant proteins also support the proposal made earlier, that τ_r of the aromatic amino acids can depend on the location of the residue in the protein structure. These ideas obviously require more study.

Finally, this work demonstrates that in studies of site-specific mutants, new concepts in the interpretation of the fluorescence of proteins relevant to their structure and dynamics are obtained. This will undoubtedly lead to new insights and information which improves the understanding of the interrelationship of protein structure, function, and dynamics.

Acknowledgments

We thank Dr. F. Ahmed for his efforts in assembling Figure 1 and for obtaining distance measurements from the oncomodulin crystal structure. We also thank Mr. S. Willie,

Division of Chemistry, NRC, for the atomic absorption measurements. The assistance of Mr. C. Hogue in the preparation of some of the oncomodulin mutant proteins and the writing of the macrotitration program for the SLM spectrofluorometer is gratefully acknowledged. The technical assistance of Mrs. R. Ball was greatly appreciated. Special acknowlegment is given to the technical expertise in the operation of the laser system and associated detection electronics of Mr. D. T. Krajcarski.

Registry No. Ca^{2+}, 7440-70-2.

References

Ahmed, F., Przybylska, M., Rose, M., Rose, D. R., Birnbaum, G. I., Pippy, M. E., & MacManus, J. P. (1990) *J. Mol. Biol. 216*, 127–140.

Andrews, L. J., & Forster, L. S. (1972) *Biochemistry 11*, 1875–1879.

Ben-Bassat, A., Bauer, K., Chang, S.-Y., Myambo, K., Boosman, A., & Chang, S. (1987) *J. Bacteriol. 169*, 751–757.

Chen, R. F. (1967) *Anal. Lett. 1*, 35–42.

Cox, J. A., Milos, M., & MacManus, J. P. (1990) *J. Biol. Chem. 265*, 6633–6637.

Donzel, B., Gauduchon, P., & Wahl, Ph. (1974) *J. Am. Chem. Soc. 96*, 801–808.

Eisinger, J. (1969) *Photochem. Photobiol. 9*, 247–258.

Golden, L. F., Corson, D. C., Sykes, B. D., Banville, D., & MacManus, J. P. (1989) *J. Biol. Chem. 264*, 20314–20319.

Haiech, J., Klee, C. B., & Demaille, J. G. (1981) *Biochemistry 20*, 3890–3897.

Hapak, R. C., Lammers, P. J., Palmisano, W. A., Birnbaum, E. R., & Henzyl, M. T. (1989) *J. Biol. Chem. 264*, 18751–18760.

Hutnik, C. M. L., & Szabo, A. G. (1989) *Biochemistry 28*, 3923–3934.

Hutnik, C. M. L., MacManus, J. P., Banville, D., & Szabo, A. G. (1990a) *J. Biol. Chem. 265*, 11456–11464.

Hutnik, C. M. L., MacManus, J. P., & Szabo, A. G. (1990b) *Biochemistry 29*, 7318–7328.

Ilich, P., Axelson, P. H., & Prendergast, F. G. (1988) *Biophys. Chem. 29*, 341–349.

Kilhoffer, M.-C., Demaille, J. G., & Gerard, D. (1981) *Biochemistry 20*, 4407–4414.

Knutson, J. R., Walbridge, D. G., & Brand, L. (1982) *Biochemistry 21*, 4671–4679.

MacManus, J. P. (1980) *Biochim. Biophys. Acta 621*, 296–304.

MacManus, J. P. & Whitfield, R. F. (1983) *Calcium Cell Funct. 4*, 411–440.

MacManus, J. P., Boynton, A. L., & Whitfield, J. F. (1978) *Adv. Cyclic Nucleotide Res. 9*, 485–491.

MacManus, J. P., Watson, D. C., & Yaguchi, M. (1983) *Eur. J. Biochem. 136*, 9–17.

MacManus, J. P., Szabo, A. G., & Williams, R. E. (1984) *Biochem. J. 220*, 261–268.

MacManus, J. P., Brewer, L. M., & Whitfield, J. F. (1985) *Cancer Lett. 27*, 145–151.

MacManus, J. P., Hutnik, C. M. L., Sykes, B. D., Szabo, A. G., Williams, T. C., & Banville, D. (1989) *J. Biol. Chem. 264*, 3470–3477.

McKinnon, A. E., Szabo, A. G., & Miller, D. R. (1977) *J. Phys. Chem. 81*, 1564–1570.

Privat, J. P., Wahl, P., & Auchet, J. C. (1979) *Biophys. Chem. 9*, 223–233.

Schauerte, J. A., & Gafni, A. (1989) *Biochemistry 28*, 3948–3954.

Szabo, A. G. (1990) in *Protein Engineering* (Narang, S, A., Ed.) pp 159–186, Butterworths, New York.

Van Durren, B. L. (1961) *J. Org. Chem. 26*, 2954.

Whitfield, J. F., Boynton, A. L., MacManus, J. P., Rixon, R. H., Sikorska, M., Tsjang, B. K., Walker, P. R., & Swierenga, S. H. H. (1980) *Ann. N.Y. Acad. Sci. 339*, 216–240.

Willis, K. J., & Szabo, A. G. (1989) *Biochemistry 28*, 4902–4908.

Willis, K. J., & Szabo, A. G. (1991) *J. Phys. Chem. 95*, 1585–1589.

Zamyatnin, A. A. (1972) *Prog. Biophys. Mol. Biol. 24* 107–123.